



# Ion dynamics in quasi-perpendicular collisionless interplanetary shocks: a case study

Michael Gedalin<sup>1\*</sup> and Wolfgang Dröge<sup>2</sup>

<sup>1</sup> Department of Physics, Ben Gurion University of the Negev, Beer-Sheva, Israel

<sup>2</sup> Lehrstuhl für Astronomie, University of Würzburg, Würzburg, Germany

## Edited by:

Rudolf A. Treumann, Munich University, Germany

## Reviewed by:

Rudolf A. Treumann, Munich University, Germany  
Mark E. Dieckmann, Linköping University, Sweden

## \*Correspondence:

Michael Gedalin, Department of Physics, Ben Gurion University of the Negev, Beer-Sheva 84105, Israel  
e-mail: gedalin@bgu.ac.il

Interplanetary shocks are believed to play an important role in the acceleration of charged particles in the heliosphere. While the acceleration to high energies proceeds via the diffusive mechanism at the scales exceeding by far the shock width, the initial stage (injection) should occur at the shock itself. Numerical tracing of ions is done in a model quasi-perpendicular shock front with a typical interplanetary shock parameters (Mach number, upstream ion temperature). The analysis of the distribution of the transmitted solar wind is used to adjust the cross-shock potential which is not directly measured. It is found that, for typical upstream ion temperatures, acceleration of the ions from the tail of the solar wind distribution is unlikely. Pickup ions with a shell distribution are found to be effectively energized and may be injected into further diffusive acceleration regime. Pre-accelerated ions are efficiently upscaled in energies. A part of these ions is returned to the upstream region where they can further be diffusively accelerated.

**Keywords:** collisionless shocks, particle acceleration, non-linear waves, ion dynamics, heliospheric shocks

## 1. INTRODUCTION

Collisionless shocks are believed to be most efficient particle accelerators in the plasma universe. These shocks are present in virtually all space systems and are formed whenever a high velocity (super-magneto-sonic) flow is decelerated by an obstacle or when a super-magneto-sonic blast waver propagates in an ambient plasma. When viewed in the reference frame, moving with the shock, the energy of the directed flow of incident ions is re-distributed to these ions themselves (in the form of the heating of the bulk of the ion distribution and acceleration of a typically small fraction of those), to the electrons (heating and acceleration), and fields (enhancement of the magnetic field in fast shocks). Thus, the incident (upstream) ions are the source of all energy available to the shock to be released in other forms. Therefore, ion dynamics in the shock front is of utmost importance for understanding of the shock physics. In quasi-perpendicular shocks, which have a well-defined spatial structure, even when they are not exactly one-dimensional and stationary, the ion motion across the shock front is determined by the macroscopic magnetic and electric fields inside the shock and only weakly affected by superimposed wave activity. Indeed, the overall shock width, including the magnetic foot, the ramp, and the overshoot is smaller than the upstream ion convective gyroradius. The width of the steepest magnetic field jump, the ramp, is *much* smaller than the convective gyroradius [24, 37, 42], which means that the time a typical ion spends in this region is a small part of the ion gyroperiod. At this time scale any influence of the transient waves should be negligible. Yet, there is always a minority of ions which remain for a long time in the ramp vicinity, and these ions may be affected by the ramp non-stationarity [48]. Although some of observed shocks have been found to be non-stationary [28, 30, 34] or rippled [35, 37], it is

not clear yet what fraction of shocks and in what parameter range substantially differ from a simple planar structure due to ripples propagating along the shock front [8, 9, 31, 39], while numerical simulations of the shock reformation mechanisms are still debated [12, 25, 29, 32].

In the present paper we restrict ourselves to the ion dynamics in the one-dimension and stationary shock structure, leaving the analysis of the effects of the rippling and/or non-stationarity for elsewhere [21, 44, 49]. Despite these limitations, the ion dynamics is rich, and the macroscopic fields were shown to be responsible for a number of phenomena: ion reflection at the shock front [10, 19, 46], production of backstreaming ions [22, 33], acceleration of pickup ions [1, 11, 27, 50], and formation of the downstream gyrating distributions and magnetic oscillations [5, 38, 39, 43].

Unless there is a substantial superthermal population of ions upstream of the shock [1], the field structure in the shock front (at least at the scales between the electron inertial scale and ion inertial scale) is intimately related to the ion distributions which are formed when the thermal solar wind protons cross the shock. Analyzing only the integral characteristics of these distributions, it is possible, in principle, to find the shock parameters which are not directly measured (like the cross-shock potential). In some cases, comparison of the numerical analysis (see below) with the observed magnetic profile alone allows to make significant conclusions [23, 52]. The shock front features at electron scales, like electric field spikes inside the ramp [2, 47] cannot be found in this way.

In the present paper we analyze the ion dynamics in a model profile of a low-Mach ( $M_A = 3$ ) shock. The objective is not to imitate nature by reproducing an observed shock but to study what parameters control the ion dynamics (transmission of solar wind ions and as well as acceleration of superthermal ion) at the

shock front. Thus, our approach is manifestly not self-consistent since we start with an analytical model for the magnetic profile (not with a fit to an observed shock). Yet, we succeed to fit a number of parameters (cross-shock potential, ramp width) so that the magnetic profile which would be consistent with the ion distributions, derived numerically, does not differ substantially from the initial profile.

Once a shock structure is adjusted to the dynamics of the bulk of the ions, it is possible to study the behavior of the minority: the tail of the thermal distribution, the pickup ions, and the pre-accelerated seed population. Of special interest is a possible upscale of the energies of these ions as a first step toward the diffusive acceleration [6, 7, 15, 26]. In particular, ions accelerated previously at the Sun, may appear upstream of a travelling interplanetary shock [40]. An alternative would be acceleration of small number of protons from the superthermal tail of the solar wind population or from the pickup ion shell distribution. Keeping the approximate consistency of the numerically derived and analytically assumed profiles, we establish conditions on other shock parameters ( $\beta_i$ ,  $\theta$ , and cross-shock potential) which allow injection from the tail of the thermal distribution, primary acceleration of pickup ions, and upscale of the energies of a pre-accelerated seed population.

## 2. SHOCK MODEL

Typically interplanetary shocks are low to medium Mach number shocks with the Alfvénic Mach number  $\leq 4$  and fast magnetosonic Mach number  $\leq 3$  (see the IGPP/UCLA database for STEREO shocks and CFA Interplanetary Shock Database). For such shocks no significant foot or overshoot are expected so that we adopt the following simple shape for the magnetic field components:

$$b_z = \frac{B_z}{B_u} = \sin \theta b(x), \tag{1}$$

$$b(x) = \frac{R + 1}{2} + \frac{R - 1}{2} \tanh \frac{3x}{D} \tag{2}$$

$$b_x = \frac{B_x}{B_u} = \cos \theta \tag{3}$$

$$b_y = \frac{B_y}{B_u} = a \frac{db_z}{dx} \tag{4}$$

Here  $x$  is along the shock normal and  $x - z$  is the coplanarity plane. The coordinates are normalized on the upstream proton convective gyroradius,  $L_g = V_u / \Omega_u$ , where  $V_u = M_A v_A$  is the velocity of the upstream flow while  $\Omega_u = eB_u / m_i c$  is the upstream proton gyrofrequency. In the expression above the effective width of the ramp is  $2D$ . According to the statistical studies of [37] and [24] the ramp width can be expected within  $(0.1 - 0.5)(c/\omega_{pi})$ , where the ion inertial length is related to the convective gyroradius as  $c/\omega_{pi} = L_g/M_A$ . The non-coplanar magnetic field shape is chosen approximately in accordance with [17, 36]. One of the most important unknowns is the cross-shock potential. For the potential shape we use the following expression [14, 18, 20] (the energy drop is normalized on the upstream

ion energy):

$$\phi(x) = \frac{e\varphi(x)}{m_i V_u^2 / 2} = s \frac{b(x) - 1}{(R - 1)} \tag{5}$$

where  $R$  is the magnetic compression of the perpendicular component and  $s$  is the total cross-shock potential measured in the incident ion energies. The magnitude of the potential is closely related to the ion heating and formation of non-gyrotropic downstream distributions and large downstream magnetic oscillations [5, 38, 39]. For a one-dimensional stationary shock pressure balance should be maintained throughout the shock, that is,

$$p_{i,xx} + p_{e,xx} + \frac{B^2}{8\pi} = \text{const} \tag{6}$$

Here

$$p_{xx} = m \int v_x^2 f(v) dv \tag{7}$$

is the total (dynamic and kinetic) pressure. When normalizing on the upstream dynamic ion pressure  $n_u m_i V_u^2$  one gets

$$1 + \frac{1 + \beta_i + \beta_e}{2M^2} = \frac{p_{id,xx} + p_{ed,xx}}{n_u m_i V_u^2} + \frac{(B_d/B_u)^2}{2M^2} \tag{8}$$

Approximating the electron kinetic pressure (the electron dynamic pressure is negligible) as  $p_e \propto n^{\gamma}$ , one has an estimate

$$1 + \frac{1 + \beta_i + \beta_e(1 - N^{\gamma})}{2M^2} = P_{i,xx} + \frac{R_d^2}{2M^2} \tag{9}$$

where  $N = n_d/n_u$  and  $R_d = B_d/B_u$ .

In what follows we trace ions through the shock solving the equations of motion in the normalized form:

$$\dot{x} = v_x, \quad \dot{y} = v_y, \quad \dot{z} = v_z, \tag{10}$$

$$\dot{v}_x = e_x + v_y b_z - v_z b_y \tag{11}$$

$$\dot{v}_y = \sin \theta + v_z \cos \theta - v_x b_z \tag{12}$$

$$\dot{v}_z = v_x b_y - v_y \cos \theta \tag{13}$$

where  $E_x = -d\phi/dx$  and  $e_x = E_x/(V_u B_u/c)$ . We shall present the phase space distribution of ions at their first crossing of certain positions well upstream and well downstream of the ramp, at the distances exceeding the gyroradii of the ions. In addition, we will present the energy distributions derived by collecting ions over sufficiently large regions to average out the non-gyrotropy. The distribution is evaluated for 24 logarithmically spaced energy channels with minimum energy of  $0.2(m_i V_u^2/2)$  and maximum energy of  $200(m_i V_u^2/2)$ .

### 3. THERMAL POPULATION

As a first step we study the behavior of a thermal upstream population. A magnetic compression  $R = 2.5$  and an Alfvénic Mach number  $M = 3$  are kept throughout, while  $\beta_i$ ,  $\theta$ ,  $D$ , and  $s$  are varied. The choice of the parameters is inspired by the shock observed by Wind on May 15, 1997. **Figure 1** shows the magnetic field calculated from the pressure balance Equation (9) with the ion distribution obtained numerically. The following parameters have been chosen:  $\theta = 80^\circ$ ,  $D = 0.2$ ,  $s = 0.5$ ,  $\beta_i = 0.4$ . Electrons are sensitive to the fine scale details of the shock front, in particular, the electric field spikes which may occur within the ramp [3, 4, 45]. Thus, they cannot be treated within the same approach. Instead, we assumed the polytropic state equation  $p_e \propto n_e^\gamma$ , with  $\gamma_e = 5/3$  and  $\beta_e = 0.6$ . It is clear that the derived magnetic field is not identical with the model field. Indeed, downstream magnetic oscillations are expected due to the non-gyrotropy of the downstream ion distribution. Numerical iterations are possible including these oscillations in the magnetic profile. Yet, the effects of these refinements are not significant for our purposes and even contradicts the principles of the approach. Given the uncertainty of our knowledge of the shock physics the agreement between the initial smooth profile and numerically derived shape is quite satisfactory. It is worthwhile to note that it is for the first time that a theoretically proposed analytical shape for the magnetic field is successfully completed with fitting a small number of the shock parameters to be consistent with the ion dynamics in the shock front. Previous studies either fitted an observed shock profile or obtained the fields in self-consistent numerical simulations where a shock formed by itself.

**Figure 2** shows the trajectories of 40 randomly chosen ions. Gradual gyrophase mixing is clearly seen. **Figure 3** shows the final energies of the ions (left panel) and the energy spectrum upstream (stars) and downstream (circles). The final energy of an ion is determined at the first crossing of a certain far upstream position or a certain far downstream position, therefore, the scatter-plot does not represent the distribution at these positions. Here and hereafter the shown energy spectra are normalized so that  $\int (dN/dE)dE = 1$ , while the ion energies are normalized on

the energy of the ion with the speed equal to the solar wind speed,  $E_u = m_i V_u^2/2$ . In this case there were no backstreaming ions. Most of the ions are directly transmitted while a small fraction are the reflected ions (those which make a loop ahead of the ramp or in the ramp itself). Using the staying time method [see, e.g., 23] the energy spectra are obtained by averaging over sufficiently large upstream and downstream regions to take into account the ion gyration. The upstream distribution is a shifted Maxwellian while the downstream distribution is not. The latter has a high energy tail due to the reflected ions, although their contribution to the total energy (or pressure) is small because of their low density.

In attempts to vary the shock parameters and maintain the consistency of the pressure balance derived shock profile with the initially chosen one we found that only moderate changes are allowed. **Figure 4** shows the derived magnetic profile for  $\theta = 70^\circ$  with other parameters unchanged. The initial and derived profiles are consistent to the same degree as in for  $\theta = 80^\circ$ . In what follows we present only significant changes which occur within the allowed variation limits of the shock parameters (the ramp width  $D$  and the angle between the shock normal and the upstream magnetic field  $\theta$ ). Within the allowed variations of the cross-shock parameters no significant changes have been found.

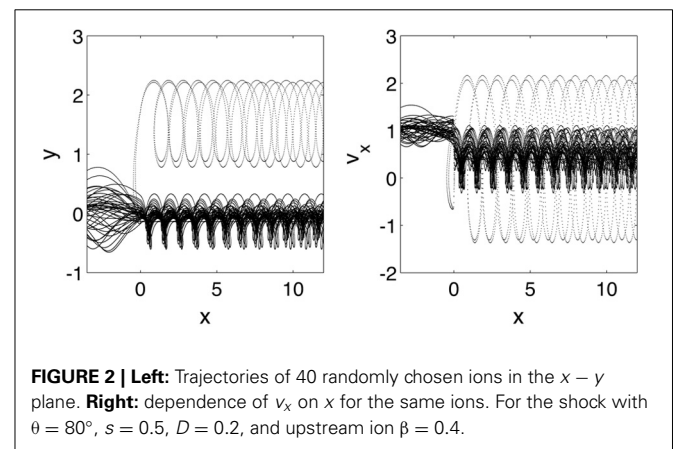


**FIGURE 2 | Left:** Trajectories of 40 randomly chosen ions in the  $x - y$  plane. **Right:** dependence of  $v_x$  on  $x$  for the same ions. For the shock with  $\theta = 80^\circ$ ,  $s = 0.5$ ,  $D = 0.2$ , and upstream ion  $\beta = 0.4$ .

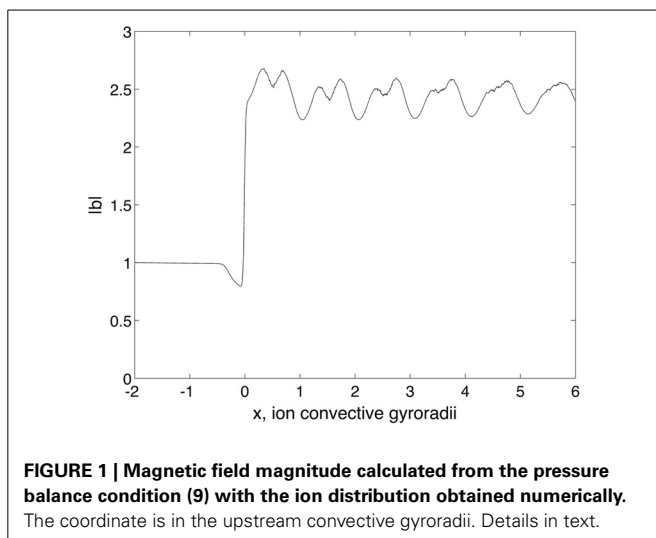


**FIGURE 1 | Magnetic field magnitude calculated from the pressure balance condition (9) with the ion distribution obtained numerically.** The coordinate is in the upstream convective gyroradii. Details in text.

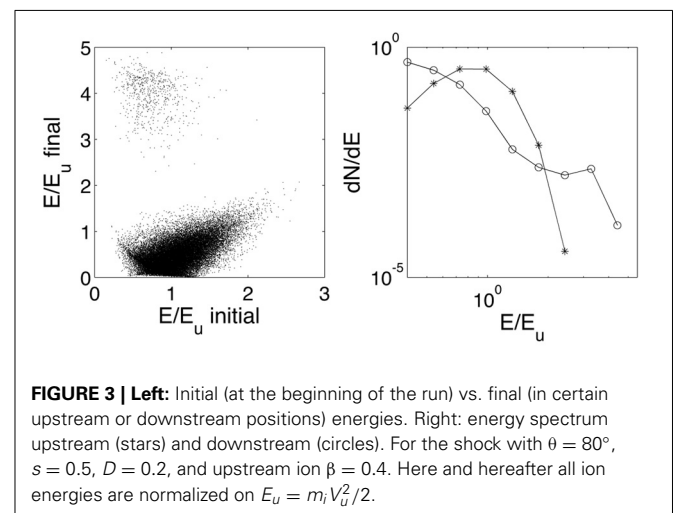


**FIGURE 3 | Left:** Initial (at the beginning of the run) vs. final (in certain upstream or downstream positions) energies. **Right:** energy spectrum upstream (stars) and downstream (circles). For the shock with  $\theta = 80^\circ$ ,  $s = 0.5$ ,  $D = 0.2$ , and upstream ion  $\beta = 0.4$ . Here and hereafter all ion energies are normalized on  $E_u = m_i V_u^2/2$ .

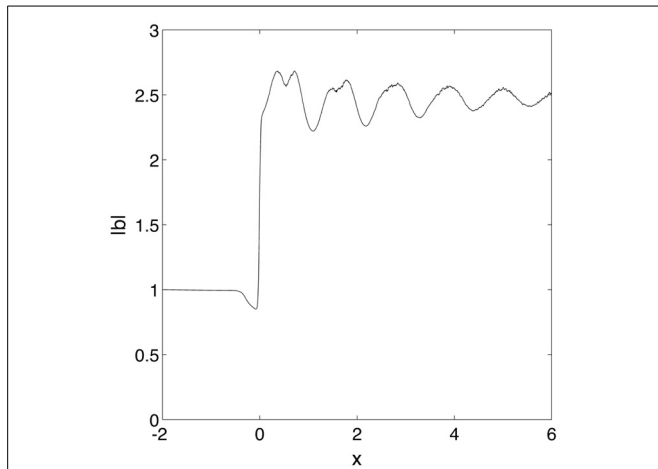


**FIGURE 4 |** Magnetic field magnitude calculated from the pressure balance condition with the ion distribution obtained numerically for  $\theta = 70^\circ$ . Other parameters remain the same as above.

#### 4. PICKUP IONS

Once the analytical profile is found to be consistent with the dynamics of the solar wind ions in the shock front and the limits of variations of the parameters, which do not break the consistency, are established, it is possible to study the motion of ions from low-density populations in this shock. Of particular interest is acceleration of superthermal ions with possible further injection to the diffusive acceleration process. Pickup ions are the natural candidates for acceleration at quasi-perpendicular shocks. They were shown theoretically to be efficiently accelerated at a plane high-Mach number shock by surfing or multiple reflections [see, e.g., 27, 50, 51]. This acceleration is consistent with the observations of energetic particles at the termination shock where the pickup ions are one of the major channels of the energy re-distribution [1, 13, 16, 41] due to their high density. The density of superthermal pickup ions in the inner heliosphere is low so that they do not affect the shock profile. Hence, we can analyze their dynamics in the shock front using the parameters established above. In the present paper we model the upstream distribution of these ions with a thin isotropic shell with the radius  $v_p = 1$  around the drift velocity  $V_u = 1$ . Thus, the initial velocities of a pickup ion is  $v_x = 1 + \sin \alpha \cos \varphi$ ,  $v_y = \sin \alpha \sin \varphi$ ,  $v_z = \cos \alpha$ , where the angles are chosen randomly and uniformly distributed in the corresponding ranges  $0 \leq \alpha \leq \pi$ ,  $0 \leq \varphi < 2\pi$ . **Figure 5** shows the final energies of the ions (left panel) and the energy spectrum upstream (stars) and downstream (circles), for  $\theta = 80^\circ$ ,  $s = 0.5$ , and  $D = 0.2$ . There are no backstreaming ions and the energization of the downstream ions is rather modest, less than by an order of magnitude.

Earlier it was shown [51] that pickup ion acceleration is greatly enhanced when the shock is thinner or a fine structure of the shock ramp is present. In order to analyze this effect we change the ramp width to  $D = 0.1$ . **Figure 6** shows the corresponding energy spectra. The acceleration is now much stronger. **Figure 7** shows trajectories of several ions and zooms in on the trajectory of the ion with maximum acceleration. It is clearly seen that the

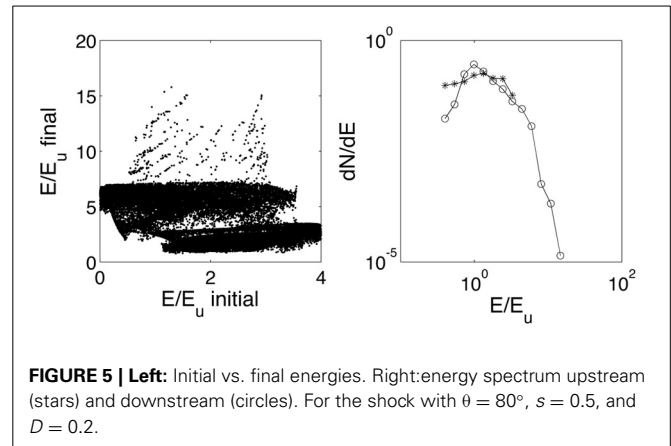


**FIGURE 5 |** Left: Initial vs. final energies. Right: energy spectrum upstream (stars) and downstream (circles). For the shock with  $\theta = 80^\circ$ ,  $s = 0.5$ , and  $D = 0.2$ .

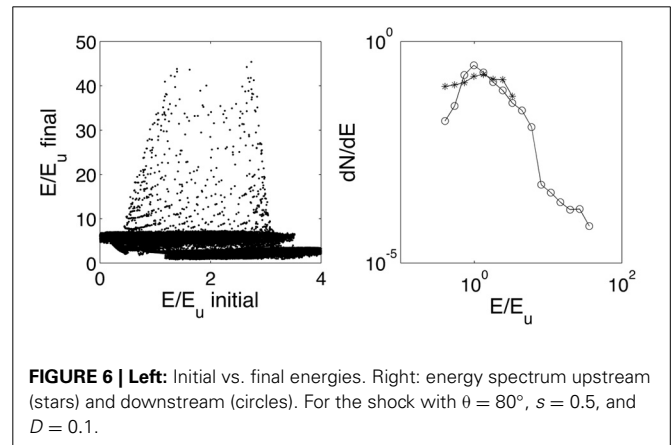


**FIGURE 6 |** Left: Initial vs. final energies. Right: energy spectrum upstream (stars) and downstream (circles). For the shock with  $\theta = 80^\circ$ ,  $s = 0.5$ , and  $D = 0.1$ .

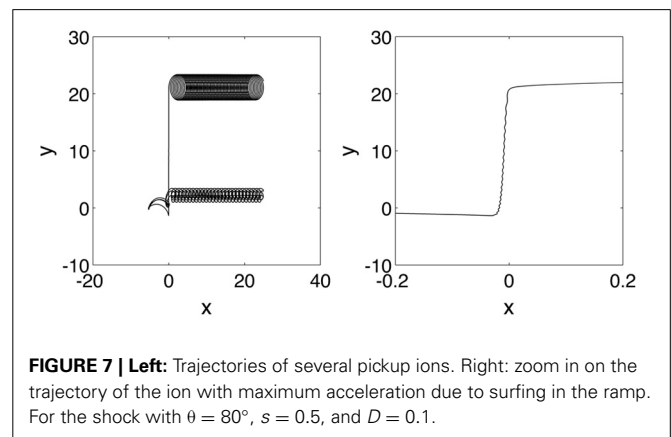


**FIGURE 7 |** Left: Trajectories of several pickup ions. Right: zoom in on the trajectory of the ion with maximum acceleration due to surfing in the ramp. For the shock with  $\theta = 80^\circ$ ,  $s = 0.5$ , and  $D = 0.1$ .

ion is accelerated due to surfing in the ramp [27, 51]. There are no backstreaming ions in this case either, which makes injection into further diffusive acceleration less plausible.

Changing the angle to  $\theta = 70^\circ$  allows some ions to escape upstream. The corresponding distributions are shown in **Figure 8**. The highest energy ions are backstreaming ions. These ions are the natural candidates for the seed population for further diffusive acceleration. **Figure 9** shows trajectories of several ions (left panel). The combination of surfing with multiple reflection [50] is clearly seen. For comparison, the right panel shows

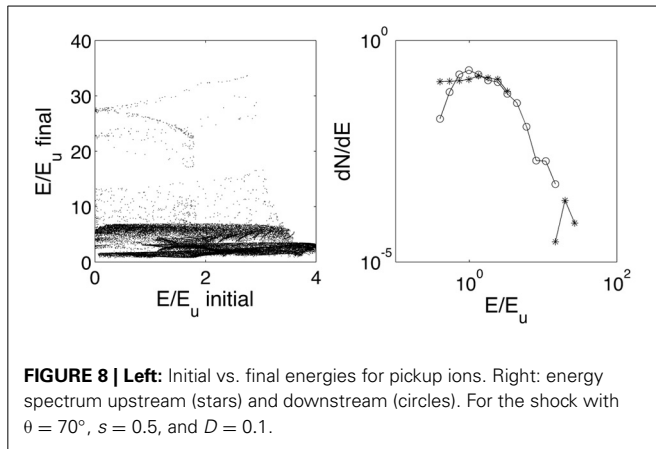


**FIGURE 8 | Left:** Initial vs. final energies for pickup ions. **Right:** energy spectrum upstream (stars) and downstream (circles). For the shock with  $\theta = 70^\circ$ ,  $s = 0.5$ , and  $D = 0.1$ .

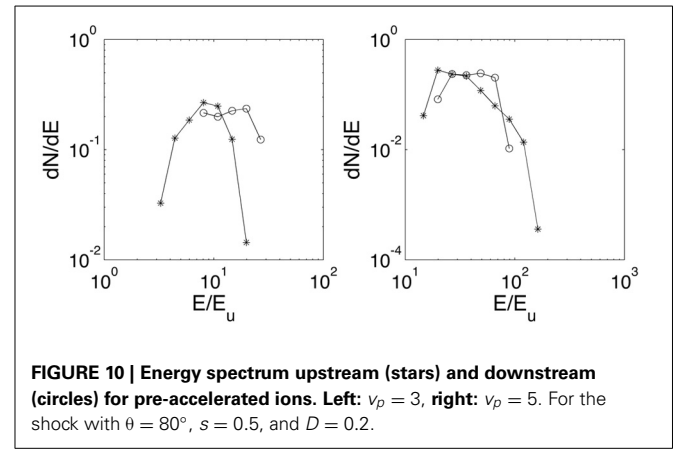


**FIGURE 10 | Energy spectrum upstream (stars) and downstream (circles) for pre-accelerated ions. Left:**  $v_p = 3$ , **right:**  $v_p = 5$ . For the shock with  $\theta = 80^\circ$ ,  $s = 0.5$ , and  $D = 0.2$ .

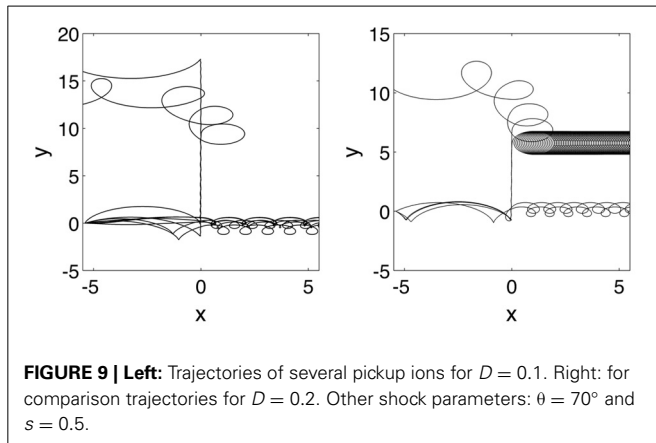


**FIGURE 9 | Left:** Trajectories of several pickup ions for  $D = 0.1$ . **Right:** for comparison trajectories for  $D = 0.2$ . Other shock parameters:  $\theta = 70^\circ$  and  $s = 0.5$ .

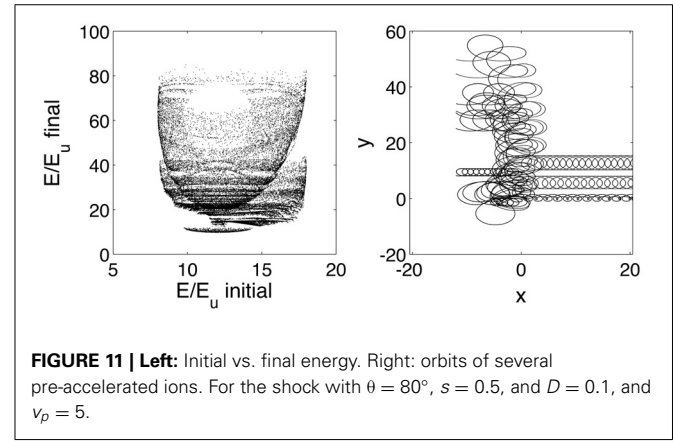


**FIGURE 11 | Left:** Initial vs. final energy. **Right:** orbits of several pre-accelerated ions. For the shock with  $\theta = 80^\circ$ ,  $s = 0.5$ , and  $D = 0.1$ , and  $v_p = 5$ .

several trajectories in the case  $D = 0.2$ . The acceleration energies are comparable and backstreaming ions are also present. The energy an ion acquires is directly related to the distance the ion moves along the shock front in the direction of the motional electric field  $E_y$ . In both cases this distance is of the order of 10 convective gyroradii. The acceleration occurs in the close vicinity of the shock front. Low- and medium-Mach number,  $M \lesssim 3$ , interplanetary shocks are not expected to be unstable to rippling at the ion convective gyroradius scale [39]. Thus, the described process is a viable mechanism of the injection. Rippling at larger scales may affect further behavior but would not change significantly the prompt acceleration at the shock front. The time scale of this acceleration is less than ten gyroperiods. Therefore, non-stationarity at smaller times would affect the ion dynamics. Upon leaving the shock transition region, these ions have substantial velocities along the magnetic field (not shown here) and keep moving in  $z$  direction. Escaping further upstream they may find themselves in the foreshock of a more oblique and even a quasi-parallel shock, where upstream turbulence may more easily scatter them back to the shock front.

## 5. PRE-ACCELERATED POPULATION

Finally, we are interested in the behavior of a pre-accelerated ion population. Such populations may be produced by another source and be brought to the upstream region of the propagating interplanetary shock [40]. Since our objective is to find out whether

it is possible to upscale the energies of the ions from such population and to produce accelerated backstreaming ions, we shall restrict ourselves with simple shell distributions with  $v_p = 3$  and  $v_p = 5$ . The corresponding distributions are shown in **Figure 10**. The initial vs. final energies and orbits are shown in **Figure 11** for the case  $v_p = 5$ . There is a substantial upscale of the energies, almost by an order of magnitude for a fraction of the ions. While the highest energy ions are downstream for  $v_p = 3$ , in the case  $v_p = 5$  the highest energy ions escape back upstream. The main acceleration process seems to be multiple reflection. In this case also the acquired energy depends on the shift along the non-coplanarity direction within the shock front. The distance the most energetic ions pass along this direction is not much larger than for pickup ions, and a large scale rippling might affect the motion. Yet, the multiply reflected ions are less sensitive to the shock rippling than the surfing ions, so that this acceleration mechanism can be expected to be robust enough. The accelerated ions also have high velocities along  $z$ -direction and may move into another part of the shock with different conditions.

## 6. CONCLUSIONS

Started with an analytical shape for the magnetic field we numerically traced solar wind ions across the shock and calculated their pressure throughout. Using the pressure balance condition, which should be valid everywhere in the shock if it is one-dimensional and stationary, we derived the magnetic fields which would be

consistent with the obtained ion distribution. By varying a small number of the shock parameters (the cross-shock potential and the ramp width) we succeeded to achieve a rather good (within about 10%) agreement between the initially assumed and the numerically derived profiles. All previous studies either used a fit to an observed profile of obtained the fields in self-consistent simulations. It is for the first time when a model theoretical profile for the fields is shown to be consistent with the ion dynamics in the shock front. We have also established the limits of the variation of the shock parameters within which the arising discrepancies between the assumed and derived fields are still within the expected uncertainties of our knowledge. This achievement allowed us to study the dynamics of low-density species without breaking the validity of the used fields and without computationally heavy simulations. While here we report a single success of this kind, we plan to further exploit this method to enlarge the parameter space where suitable analytical models can be used.

The above success allowed to trace superthermal ions without fear that the variation of the shock parameters is not legitimate as it can break the balance within the shock. The objectives of the analysis were to determine (a) whether substantial energization occurs at the shock front, (b) whether there energized particles inevitably move to the downstream region or backstreaming beams can be produced, and (c) whether moderate changes of the shock parameters (the angle between the shock normal and the upstream magnetic field in our case) would result in noticeable changes in the ion accelerated ion distributions. The analysis was concentrated on a shell distribution of pickup ions and shell distributions of pre-accelerated ions. We expect that the evolution of these incident distributions is indicative of what would happen in a more general case.

Our test particle analyses have shown that quasi-perpendicular interplanetary shocks are unlikely to be capable to provide injection directly from the thermal population. Although it cannot be excluded that some ions experience acceleration, their fraction is about  $10^{-5}$  or less, for typical values of the shock parameters. This result is related to the fact that the accelerated ions come from the tail of the distribution. The number of particles in the tail depends on the ratio of the upstream thermal velocity of the ions to the upstream flow velocity,  $v_T/V_u = \sqrt{\beta/2M^2}$ . Thus, even for large  $\beta$  the effect would be weak for sufficiently high  $M$  [cf. 22].

Pickup ions, on the other hand, may be efficiently accelerated and returned to the upstream region where they could serve as a seed population for subsequent diffusive acceleration. The efficiency of the process is higher for thin shocks and higher obliquity (smaller angle between the shock normal and the upstream magnetic field). The decrease of this angle from  $\theta = 80^\circ$  to  $\theta = 70^\circ$  resulted in lower energies of downstream ions but appearance of high-energy beams reflected toward upstream. Since pickup ions exist everywhere in the heliosphere, this result means that such acceleration may be quite ubiquitous and, possibly, provide at least the first stage of the injection.

It is expected the solar accelerated ions may find their way into the upstream region of an interplanetary shock [40]. Such pre-accelerated ions may itself become a seed population for subsequent diffusive acceleration. Injection is efficient if a noticeable energy gain occurs directly at the shock front, without any need to be scattered by magnetic fluctuations (the latter process becomes

crucial at higher energies). In addition, generation of upstream directed beams would spare, at least at this stage, the necessity to be scattered from downstream against the drift. Our analyses with two shell distributions show that most ions from a pre-accelerated population acquire substantial energies on their transfer to the downstream region. A fraction (up to several percent) may be upscaled in energies by almost an order of magnitude and returned to upstream. This process is rather robust and may easily start the diffusive acceleration.

Quantitative acceleration analysis has been done here for an interplanetary shock with a modest Mach number. Previous studies were concentrated on high-Mach number shocks. Here we show, for the first time, that interplanetary shocks are efficient prompt accelerators directly at the shock front.

The above analysis used the assumptions of the shock one-dimensionality and stationarity. Rippling at small scales would affect the pickup ion motion while rippling at large scales should be eventually taken into account when analyzing the higher energy ion dynamics. If the shock front is significantly time-dependent the ion dynamics may be also affected. Although neither rippling nor reformation are not expected at the Mach numbers typical for the interplanetary shocks (which is supported by our ability to adjust the shock profile) these issues, nevertheless, require analysis. It will be done in a separate study.

## ACKNOWLEDGMENTS

This study was supported in part by GIF Grant no. 1145/2011.

## REFERENCES

- Ariad D, Gedalin M. The role pickup ions play in the termination shock. *J Geophys Res.* (2013) **118**:2854–62. doi: 10.1002/jgra.50170
- Bale SD, Mozer FS. Measurement of large parallel and perpendicular electric fields on electron spatial scales in the terrestrial bow shock. *Phys Rev Lett.* (2007) **98**:205001. doi: 10.1103/PhysRevLett.98.205001
- Balikhin M, Gedalin M. Kinematic mechanism of electron heating in shocks: theory vs observations. *Geophys Res Lett.* (1994) **21**:841–4. doi: 10.1029/94GL00371
- Balikhin M, Gedalin M, Petrukovich M. New mechanism for electron heating in shocks. *Phys Rev Lett.* (1993) **70**:1259–62. doi: 10.1103/PhysRevLett.70.1259
- Balikhin MA, Zhang TL, Gedalin M, Ganushkina NY, Pope SA. Venus express observes a new type of shock with pure kinematic relaxation. *Geophys Res Lett.* (2008) **35**:L01103. doi: 10.1029/2007GL032495
- Balogh A, Treumann RA. *Physics of Collisionless Shocks - Space Plasma Shock Waves. ISSI Scientific Report Series.* New York, NY: Springer Science+Business Media. (2013) **12**. doi: 10.1007/978-1-4614-6099-2
- Blandford R, Eichler D. Particle acceleration at astrophysical shocks - a theory of cosmic-ray origin. *Phys Rep.* (1987) **154**:1–75. doi: 10.1016/0370-1573(87)90134-7
- Burgess D. Interpreting multipoint observations of substructure at the quasi-perpendicular bow shock: simulations. *J Geophys Res.* (2006) **111**:A10210. doi: 10.1029/2006JA011691
- Burgess D, Scholer M. Shock front instability associated with reflected ions at the perpendicular shock. *Phys Plasmas* (2007) **14**:012108. doi: 10.1063/1.2435317
- Burgess D, Wilkinson WP, Schwartz SJ. Ion distributions and thermalization at perpendicular and quasi-perpendicular supercritical collisionless shocks. *J Geophys Res.* (1989) **94**:8783–92. doi: 10.1029/JA094iA07p08783
- Burrows RH, Zank GP, Webb GM, Burlaga LF, Ness NF. Pickup ion dynamics at the heliospheric termination shock observed by VOYAGER 2. *Astrophys J.* (2010) **715**:1109–16. doi: 10.1088/0004-637X/715/2/1109
- Comișel H, Scholer M, Soucek J, Matsukiyo, S. Non-stationarity of the quasi-perpendicular bow shock: comparison between Cluster observations and simulations. *Ann Geophys.* (2011) **29**:263–74. doi: 10.5194/angeo-29-263-2011

13. Decker RB, Krimigis SM, Roelof EC, Hill ME, Armstrong TP, Gloeckler G. et al. Mediation of the solar wind termination shock by non-thermal ions. *Nature* (2008) **454**:67–70. doi: 10.1038/nature07030
14. Dimmock AP, Balikhin MA, Krasnoselskikh VV, Walker SN, Bale SD, Hobara Y. A statistical study of the cross-shock electric potential at low Mach number, quasi-perpendicular bow shock crossings using Cluster data. *J Geophys Res.* (2012) **117**:A02210. doi: 10.1029/2011JA017089
15. Drury LO. An introduction to the theory of diffusive shock acceleration of energetic particles in tenuous plasmas. *Rep Progr Phys.* (1983) **46**:973–1027. doi: 10.1088/0034-4885/46/8/002
16. Florinski V, Decker RB, le Roux JA, Zank GP. An energetic-particle-mediated termination shock observed by Voyager 2. *Geophys Res Lett.* (2009) **36**:L12101. doi: 10.1029/2009GL038423
17. Gedalin M, Noncoplanar magnetic field in the collisionless shock front. *J Geophys Res.* (1996) **101**:11153–6. doi: 10.1029/96JA00518
18. Gedalin M, Transmitted ions and ion heating in nearly perpendicular low-mach number shocks. *J Geophys Res.* (1996) **101**:15569–78. doi: 10.1029/96JA00924
19. Gedalin M. Ion reflection at the shock front revisited. *J Geophys Res.* (1996) **101**:4871–8. doi: 10.1029/95JA03669
20. Gedalin M. Ion heating in oblique low-Mach number shocks. *Geophys Res Lett.* (1997) **24**:2511–4. doi: 10.1029/97GL02524
21. Gedalin M. Influence of the rippling on the collisionless ion and electron motion in the shock front- a model study. *J Geophys Res.* (2001) **106**:21645–55. doi: 10.1029/2000JA000185
22. Gedalin M, Liverts M, Balikhin MA. Distribution of escaping ions produced by non-specular reflection at the stationary quasi-perpendicular shock front. *J Geophys Res.* (2008) **113**:A05101. doi: 10.1029/2007JA012894
23. Gedalin M, Newbury JA, Russell CT. Numerical analysis of collisionless particle motion in an observed supercritical shock front. *J Geophys Res.* (2000) **105**:105–14. doi: 10.1029/1999JA000407
24. Hobara Y, Balikhin M, Krasnoselskikh V, Gedalin M, Yamagishi H. Statistical study of the quasi-perpendicular shock ramp widths. *J Geophys Res.* (2010) **115**:A11106. doi: 10.1029/2010JA015659
25. Krasnoselskikh VV, Lembège B, Savoini P, Lobzin VV. Nonstationarity of strong collisionless quasiperpendicular shocks: theory and full particle numerical simulations. *Phys Plasmas* (2002) **9**:1192–209. doi: 10.1063/1.1457465
26. Lee MA, Fisk LA. Shock acceleration of energetic particles in the heliosphere. *Space Sci. Rev.* (1982) **32**:205–28. doi: 10.1007/BF00225185
27. Lee MA, Shapiro VD, Sagdeev RZ. Pickup ion energization by shock surfing. *J Geophys Res.* (1996) **101**:4777–89. doi: 10.1029/95JA03570
28. Lefebvre B, Seki Y, Schwartz SJ, Mazelle C, Lucek EA. Reformation of an oblique shock observed by Cluster. *J Geophys Res.* (2009) **114**:A11107.
29. Lembège B, Savoini P, Hellinger P, Trávníček PM. Nonstationarity of a two-dimensional perpendicular shock: competing mechanisms. *J Geophys Res.* (2009) **114**:A03217.
30. Lobzin VV, Krasnoselskikh VV, Bosqued JM, Pinçon JL, Schwartz SJ, Dunlop M. Nonstationarity and reformation of high-mach-number quasiperpendicular shocks: cluster observations. *Geophys Res Lett.* (2007) **34**:L05107. doi: 10.1029/2006GL029095
31. Lowe RE, Burgess D. The properties and causes of rippling in quasi-perpendicular collisionless shock fronts. *Ann. Geophys.* (2003) **21**:671–9. doi: 10.5194/angeo-21-671-2003
32. Matsukiyo S, Scholer M. On reformation of quasi-perpendicular collisionless shocks. *Adv Space Res.* (2006) **38**:57–63. doi: 10.1016/j.asr.2004.08.012
33. Meziane K, Wilber M, Mazelle C, Parks GK, Hamza AM. A review of field-aligned beams observed upstream of the bow shock. In: Li G, Zank GP, Russell, CT. editors *The Physics of Collisionless Shocks: 4th Annual IGPP International Astrophysics Conference*, Vol. 781 of New York, NY: American Institute of Physics. (2005) 116–22.
34. Mazelle C, Lembège B, Morgenthaler A, Meziane K, Horbury TS, Génot V, et al. Self-Reformation of the Quasi-Perpendicular Shock: CLUSTER Observations. *Twelfth International Solar Wind Conference*, New York, NY: American Institute of Physics. (2010) **1216**:471–4.
35. Moullard O, Burgess D, Horbury TS, Lucek EA. Ripples observed on the surface of the Earth's quasi-perpendicular bow shock. *J Geophys Res.* (2006) **111**:A09113. doi: 10.1029/2005JA011594
36. Newbury JA, Russell CT, Gedalin M. The determination of shock ramp width using the noncoplanar magnetic field component. *Geophys Res Lett.* (1997) **24**:1975–8. doi: 10.1029/97GL01977
37. Newbury JA, Russell CT, Gedalin M. The ramp widths of high-Mach-number, quasi-perpendicular collisionless shocks. *J Geophys Res.* (1998) **103**:29581–93. doi: 10.1029/1998JA000024
38. Ofman L, Balikhin M, Russell CT, Gedalin M. Collisionless relaxation of ion distributions downstream of laminar quasi-perpendicular shocks. *J Geophys Res.* (2009) **114**:A09106. doi: 10.1029/2009JA014365
39. Ofman L, Gedalin M. Two-dimensional hybrid simulations of quasi-perpendicular collisionless shock dynamics: gyrating downstream ion distributions. *J Geophys Res.* (2013) **118**:1828–36. doi: 10.1029/2012JA018188
40. Reames DV. The two sources of solar energetic particles. *Space Sci Rev.* (2013) **175**:1–4. doi: 10.1007/s11214-013-9958-9
41. Richardson JD, Kasper JC, Wang C, Belcher JW, Lazarus AJ. Cool heliosheath plasma and deceleration of the upstream solar wind at the termination shock. *Nature* (2008) **454**:63–6. doi: 10.1038/nature07024
42. Russell CT, Hoppe MM, Livesey WA, Gosling JT, Bame SJ. ISEE-1 and-2 observations of laminar bow shocks- velocity and thickness. *Geophys Res Lett.* (1982) **9**:1171–4. doi: 10.1029/GL009i010p01171
43. Russell CT, Jian LK, Blanco-Cano X, Luhmann JG. Stereo observations of upstream and downstream waves at low mach number shocks. *Geophys Res Lett.* (2009) **36**:L03106. doi: 10.1029/2008GL036991
44. Scholer M, Shinohara I, Matsukiyo S. Quasi-perpendicular shocks: length scale of the cross-shock potential, shock reformation, and implication for shock surfing. *J Geophys Res.* (2003) **108**:1014. doi: 10.1029/2002JA009515
45. Schwartz SJ, Henley E, Mitchell J, Krasnoselskikh V. Electron temperature gradient scale at collisionless shocks. *Phys Rev L.* (2011) **107**:215002. doi: 10.1103/PhysRevLett.107.215002
46. Sckopke N, Paschmann G, Bame SJ, Gosling JT, Russell CT. Evolution of ion distributions across the nearly perpendicular bow shock - Specularly and non-specularly reflected-gyrating ions. *J Geophys Res.* (1983) **88**:6121–36. doi: 10.1029/JA088iA08p06121
47. Walker S, Alleyne H, Balikhin M, André M, Horbury T. Electric field scales at quasi-perpendicular shocks. *Ann Geophys.* (2004) **22**:2291–300. doi: 10.5194/angeo-22-2291-2004
48. Yang ZW, Lembège B, Lu QM. Impact of the nonstationarity of a supercritical perpendicular collisionless shock on the dynamics and energy spectra of pickup ions. *J Geophys Res.* (2011) **116**:A08216. doi: 10.1029/2010JA016360
49. Yang ZW, Lembège B, Lu QM. Impact of the rippling of a perpendicular shock front on ion dynamics. *J Geophys Res.* (2012) **117**:07222. doi: 10.1029/2011JA017211
50. Zank GP, Pauls HL, Cairns IH, Webb GM. Interstellar pickup ions and quasi-perpendicular shocks: implications for the termination shock and interplanetary shocks. *J Geophys Res.* (1996) **101**:457–77. doi: 10.1029/95JA02860
51. Zilbersher D, Gedalin M. Pickup ion dynamics at the structured quasi-perpendicular shock. *Planet Space Sci.* (1997) **45**:693–703. doi: 10.1016/S0032-0633(97)00030-5
52. Zilbersher D, Gedalin M, Newbury JA, Russell CT. Direct numerical testing of stationary shock model with low mach number shock observations. *J Geophys Res.* (1998) **103**:26775–82. doi: 10.1029/98JA02464

**Conflict of Interest Statement:** The authors declare that the research was conducted in the absence of any commercial or financial relationships that could be construed as a potential conflict of interest.

Received: 03 October 2013; accepted: 26 November 2013; published online: 13 December 2013.

Citation: Gedalin M and Dröge W (2013) Ion dynamics in quasi-perpendicular collisionless interplanetary shocks: a case study. *Front. Physics* 1:29. doi: 10.3389/fphy.2013.00029

This article was submitted to *Space Physics*, a section of the journal *Frontiers in Physics*.

Copyright © 2013 Gedalin and Dröge. This is an open-access article distributed under the terms of the Creative Commons Attribution License (CC BY). The use, distribution or reproduction in other forums is permitted, provided the original author(s) or licensor are credited and that the original publication in this journal is cited, in accordance with accepted academic practice. No use, distribution or reproduction is permitted which does not comply with these terms.